Magnetohydrodynamic Flow Between a Solid Rotating Disk and a Porous Stationary Disk

S.K. Kumar
W.I. Thacker
L.T. Watson

TR 87-6

MAGNETOHYDRODYNAMIC FLOW BETWEEN A SOLID ROTATING DISK AND A POROUS STATIONARY DISK

S. Kishore Kumar†
Director's Unit
National Aeronautical Laboratory
Bangalore, India 560 017

William I. Thacker
Computer Science
Winthrop College
Rock Hill, South Carolina 29733

Layne T. Watson‡
Department of Computer Science
Virginia Polytechnic Institute and State University
Blacksburg, Virginia 24061

Abstract. In this paper we examine the flow of a conducting fluid between a solid rotating disk and a stationary porous disk with uniform injection of fluid through the porous disk in the presence of an axial magnetic field. The equations of motion are solved using least change secant update quasi-Newton and modern root finding techniques. The fluid motion depends on the cross-flow Reynolds number, rotational Reynolds number and Hartmann number. The effects of the parameters on the flow field are presented graphically.

1. INTRODUCTION

The Navier-Stokes equations for the steady incompressible flow between two infinite coaxial disks are amenable to similarity transformations. In the context of hydrodynamics, Batchelor [1] used similarity transformations to qualitatively study the solution for different ranges of Reynolds numbers R_1 and R_2 based upon the angular velocities of the disks and the gap length, respectively. Stewartson [2] obtained a series solution for small values of R_1 and R_2. Several later investigations [3]–[6] used analytical and numerical techniques. The flow between rotating disks with injection on the porous disk was throughly examined by Wang and Watson [7]. Several other references can be found in [7].

Srivasthava and Sharma [8] extended the solid rotating disks problem to MHD flow obtaining a solution for rotational Reynolds number $R_1 << 1$. This problem was analyzed analytically and numerically by Stephenson [9] for arbitrary Reynolds number R and Hartmann number M. Chandrasekhara and Rudriah [10] obtained solutions for the two dimensional stationary case with small suction and injection velocities. Later Chandrasekhara and Rudriah [11] studied the case of axisymmetric flow between a rotating porous disk and a stationary porous disk with suction and

† The work of this author was supported by a fellowship from CSIR, Delhi.
‡ The work of this author was supported in part by Air Force Office of Scientific Research Grant 85–0250.

injection, restricting the rotation and magnetic field parameters. Recently, Agarwal and Bhargava [12] studied numerically the flow between a solid rotating and a stationary porous disk with suction.

This paper examines the flow of a conducting fluid between a solid rotating and a stationary porous disk. At the stationary porous disk, fluid is injected with uniform velocity w. By using suitable similarity transformations, the governing nonlinear partial differential equations are reduced to nonlinear ordinary differential equations. These equations are solved numerically using a least change secant update quasi-Newton and modern root finding methods. The problem depends on the nondimensional parameters R, R_1 and M which are the cross-flow Reynolds number, rotational Reynolds number and Hartmann number respectively. The effects of these parameters on the flow field are shown graphically.

2. FORMULATION OF THE PROBLEM

Consider the flow of an incompressible fluid of density ρ, viscosity μ and electrical conductivity σ bounded by two coaxial disks at $z = 0$ and $z = h$ using a cylindrical polar coordinate system (r, θ, z). The z-axis is the axis of the disks. The upper disk at $z = h$ is rotating at a constant angular velocity Ω. The lower stationary porous disk has fluid injected with a uniform velocity w. A uniform magnetic field of strength B_0 is imposed in the z direction. In the analysis of this problem it is assumed that the distance h between the two disks is small compared to the radius, r_0, of the disks and that the edge effects are negligible.

The governing magnetohydrodynamic (MHD) equations of motion for the steady flow [9] are

$$\rho(\vec{q}\cdot\nabla)\vec{q} = -\nabla p + \mu\nabla^2\vec{q} + \vec{J}\times\vec{B}, \tag{1}$$
$$\nabla\cdot\vec{q} = 0, \tag{2}$$
$$\nabla\cdot\vec{B} = 0, \tag{3}$$
$$\nabla\times\vec{B} = \mu_m\sigma(\vec{E} + \vec{q}\times\vec{B}), \tag{4}$$
$$\nabla\times\vec{E} = 0, \tag{5}$$
$$J = \sigma(\vec{E} + \vec{q}\times\vec{B}), \tag{6}$$
$$\nabla\cdot\vec{J} = 0, \tag{7}$$

where ∇ and ∇^2 are the standard gradient and Laplacian operators expressed in cylindrical co-ordinates, and where $\vec{q}=(u_r, u_\theta, u_z)$, $\vec{J}=(J_r, J_\theta, J_z)$, $\vec{B}=(0, 0, B_0)$, $\vec{E}=(E_r, E_\theta, E_z)$, μ_m and p are the velocity field, current density, magnetic field, electric field, magnetic permeability and pressure respectively. The components of the vectors refer to the r, θ and z directions respectively.

For axisymmetric flow, equation (5) gives

$$E_\theta = 0. \tag{8}$$

Assume that the induced magnetic field is small compared to the imposed magnetic field. This gives

$$\vec{B} = \hat{z}B_0.$$

where $\hat{z}$ is the unit vector in the direction of the positive z-axis.

Using these approximations, equation (6) gives

$$J_\theta = -\sigma B_0 u_r, \tag{9}$$
$$J_z = \sigma E_z. \tag{10}$$

Assuming

$$E_r = -\chi B_0 \Omega r \tag{11}$$

yields

$$J_r = \sigma B_0 (u_\theta - \chi \Omega r), \tag{12}$$

where χ is a dimensionless quantity denoting the strength of the induced radial electric field and is equal to ω_{av}/Ω for insulated disks. ω_{av} is the average velocity of the fluid.

Using the equations of motion (1) and (2), assuming the flow is axisymmetric, and incorporating equations (8), (9), (10) and (12) (see Stephenson [9]) yields

$$\frac{\partial}{\partial r}(r u_r) + \frac{\partial}{\partial z}(r u_z) = 0, \tag{13}$$
$$u_r \frac{\partial u_r}{\partial r} + u_z \frac{\partial u_r}{\partial z} - \frac{u_\theta^2}{r} = -\frac{1}{\rho}\frac{\partial p}{\partial r} + \nu\left(\nabla^2 u_r - \frac{u_r}{r^2}\right) - \frac{\sigma B_0^2 u_r}{\rho}, \tag{14}$$
$$\frac{u_r}{r}\frac{\partial}{\partial r}(r u_\theta) + u_z \frac{\partial u_\theta}{\partial z} = \nu\left(\nabla^2 u_\theta - \frac{u_\theta}{r^2}\right) - \frac{\sigma B_0^2}{\rho}(u_\theta - \chi \Omega r), \tag{15}$$
$$u_r \frac{\partial u_z}{\partial r} + u_z \frac{\partial u_z}{\partial z} = -\frac{1}{\rho}\frac{\partial p}{\partial z} + \nu \nabla^2 u_z, \tag{16}$$

where

$$\nabla^2 = \frac{\partial^2}{\partial r^2} + \frac{1}{r}\frac{\partial}{\partial r} + \frac{1}{r^2}\frac{\partial^2}{\partial \theta^2} + \frac{\partial^2}{\partial z^2}$$

and $\nu = \mu/\rho$ is the kinematic viscosity. Writing $u = u(r,z)$ and $p = p(r,z)$, the boundary conditions are:

$$\begin{aligned} &u_r(r,0) = 0, \quad u_\theta(r,0) = 0, \quad u_z(r,0) = w,\\ &u_r(r,h) = 0, \quad u_\theta(r,h) = \Omega r, \quad u_z(r,h) = 0. \end{aligned} \tag{17}$$

Using the following similarity transformations:

$$\eta = \frac{z}{h}, \quad u_r = \frac{w r f'(\eta)}{2h}, \quad u_\theta = \Omega r g(\eta), \quad u_z = -w f(\eta),$$
$$p = -\rho r^2 \frac{A w^2}{4h^2} + P(\eta),$$

equations (13)–(16) reduce to

$$f''' = R\big((f')^2/2 - f f'' - \lambda g^2 - A\big) + M^2 f', \tag{18}$$
$$g'' = R(f'g - f g') + M^2 (g - \chi), \tag{19}$$
$$P = \rho\left(\frac{w^2}{2} - \frac{w^2}{2} f^2 - \frac{\nu w}{h} f'\right) + P_0.$$

The constant P_0 is the pressure at the porous stationary disk, A is a constant of integration,

$$R_1 = \Omega\frac{h^2}{\nu}, \quad R = \frac{wh}{\nu}, \quad M = B_0 h\left(\frac{\sigma}{\rho\nu}\right)^{1/2}, \quad \lambda = 2\frac{R_1^2}{R^2},$$

and

$$\chi = \int_0^1 g(\eta)\, d\eta. \tag{20}$$

The boundary conditions (17) reduce to

$$f(0) = -1, \quad f'(0) = 0, \quad g(0) = 0, \tag{21}$$

$$f(1) = 0, \quad f'(1) = 0, \quad g(1) = 1. \tag{22}$$

Differentiating equation (18) with respect to η to remove the constant A gives

$$f^{(4)} = -R(ff''' + 2\lambda gg') + M^2 f''. \tag{23}$$

3. LIFT AND TORQUE

Letting the pressure at the edge of the disk (at $r = r_0$) be p_e, the similarity transformation for p yields

$$p - p_e = -\rho(r^2 - r_0^2)\frac{Aw^2}{4h^2}.$$

The lift force is

$$L = 2\pi\int_0^{r_0}(p - p_e)r\,dr = \frac{\pi\rho w^2 r_0^4 A}{8h^2},$$

the shear stress is

$$\tau_{z\theta} = \mu\frac{\partial u_\theta}{\partial z} = \frac{\mu\Omega}{h} r g'(\eta),$$

and the torque is

$$T = 2\pi\int_0^{r_0}\tau_{z\theta} r^2\,dr = \frac{\pi\rho\nu\Omega g'(\eta)}{2h} r_0^4.$$

4. NUMERICAL METHOD

Following the format in Heruska [13], define

$$\hat{X} = \begin{pmatrix} f''(0) \\ f'''(0) \\ g'(0) \end{pmatrix}. \tag{24}$$

Let $f(\eta;\hat{X})$, $g(\eta;\hat{X})$ be the solution of the initial value problem given by (19) and (23) with initial conditions (21) and (24), where χ is treated as a constant. The original two-point boundary value problem described by equations (19) and (21)–(23) is numerically equivalent to solving the nonlinear system of equations

$$\hat{F}(\hat{X}) = \begin{pmatrix} f(1;\hat{X}) \\ f'(1;\hat{X}) \\ g(1;\hat{X}) - 1 \end{pmatrix} = 0 \tag{25}$$

together with satisfying (20). Solving (25) amounts to shooting from $\eta = 0$ to $\eta = 1$, until an appropriate value of $\hat{X}$ is determined such that the boundary conditions at $\eta = 1$ are met. However, shooting from $\eta = 0$ to $\eta = 1$ proved unsuccessful on this problem, due to the initial slope of one of the functions (f') being very large. Next, a multiple shooting technique was tried. For this define

$$X = \begin{pmatrix} f(.5) \\ f'(.5) \\ f''(.5) \\ f'''(.5) \\ g(.5) \\ g'(.5) \end{pmatrix}. \tag{26}$$

Then the boundary conditions (21) and (22) give the following nonlinear system of equations

$$F(X) = \begin{pmatrix} f(0;X) + 1 \\ f'(0;X) \\ g(0;X) \\ f(1;X) \\ f'(1;X) \\ g(1;X) - 1 \end{pmatrix} = 0. \tag{27}$$

Define

$$Y(\eta) = (f(\eta), f'(\eta), f''(\eta), f'''(\eta), g(\eta), g'(\eta)),$$

so that the value of $F(X)$ is determined from $Y(\eta)$ at $\eta = 0$ and $\eta = 1$. The vector $Y(\eta)$ can be calculated from the first order system of ordinary differential equations

$$\begin{aligned} Y_1' &= Y_2, \\ Y_2' &= Y_3, \\ Y_3' &= Y_4, \\ Y_4' &= M^2 Y_3 - R(Y_1 Y_4 + 2\lambda Y_5 Y_6), \\ Y_5' &= Y_6, \\ Y_6' &= M^2 (Y_5 - \chi) - R(Y_1 Y_6 - Y_2 Y_5), \end{aligned} \tag{28}$$

with initial conditions $Y(.5) = X$, by integrating both forward and backward. An unusual aspect of this problem is the constant χ in (20). This constant's value depends on the solution, specifically, the function $g(\eta)$. In order to satisfy (20), g must be viewed as a function of X and χ as well as η. Thus the problem is to find the value of χ such that

$$\Psi(\chi) = \int_0^1 g(\eta; X, \chi)\, d\eta - \chi = 0 \tag{29}$$

and (27) is also satisfied. To solve this problem, a least change secant update quasi-Newton method was utilized for the nonlinear system part (27) and a hybrid secant and bisection technique was utilized for the root finding part (29). The quasi-Newton code used was HYBRD from the MINPACK subroutine package from Argonne National Laboratory [14]. The root finding code used was ROOT from the ODE subroutine package in Shampine and Gordon [15]. Using an initial guess for χ, HYBRD determined an X satisfying (27). The value of $\Psi(\chi)$ using this X typically would not satisfy (29). The root finding routine used this value of $\Psi(\chi)$ to predict the root χ. This iteration was continued until (29) was satisfied.

M^2	R	R_1	χ	$g'(0)$	$g'(1)$	A
0	2	.447	.36562	.333	1.745	7.649
16	2	.447	.39460	1.237	2.777	16.946
64	2	.447	.42837	3.003	4.696	43.970
256	2	.447	.45881	6.883	8.711	147.434
512	2	.447	.46972	10.159	12.035	281.918
16	2	2.000	.39429	1.236	2.782	16.625
16	2	4.000	.39334	1.233	2.796	15.623
16	2	10.000	.38710	1.216	2.894	8.964
16	2	16.000	.37715	1.189	3.056	-2.029
16	2	2.000	.39429	1.236	2.782	16.625
16	4	2.000	.32659	.797	3.302	9.259
16	10	2.000	.22113	.305	4.392	4.853
16	16	2.000	.17273	.161	5.187	3.805

Table 1. Effects of M^2, R and R_1 on χ, $g'(0)$, $g'(1)$ and A.

5. DISCUSSION

Figure 1 shows the effect of the Hartmann number (M) on the axial, radial and tangential velocities for a fixed R and R_1. From Figure 1a, the axial velocity f is always upward. The axial velocity decreases with increased M up to just past the midplane, but increases with increased M in the upper part of the plane. The radial velocity f' is shown in Figure 1b. The radial velocity has a maximum value near the midplane of the disks for $M^2 < 64$. For larger values of M^2, the radial velocity reaches a maximum nearer the lower disk, levels off for a distance and falls to zero at the upper disk. The tangential velocity g (Figure 1c) increases as M^2 increases for $\eta < .6$ but decreases in the area closer to the upper disk as M^2 increases.

Figure 2 shows the effect of R_1 on the axial, radial and tangential velocities for a fixed M and R. Again the axial velocity is always upward (Figure 2a). Increasing R_1 has the effect of increasing the axial velocity. The effect of increasing R_1 on radial velocity (Figure 2b) is to move the maximum value towards the upper disk. Also, the maximum value is increased slightly. The effect of increasing R_1 on tangential velocity (Figure 2c) is to slightly decrease it.

Figure 3 shows the effect of R on the axial, radial and tangential velocities for a fixed M and R_1. Increasing R also increases the axial velocity (Figure 3a), but with a less pronounced effect than increasing R_1. There is less effect on radial velocity (Figure 3b) for large values of R than R_1. However, changes in small values of R have more effect on radial velocity than changes in small values of R_1. The tangential velocity (Figure 3c) is effected by changes in R significantly, unlike changes in R_1. The effect of increasing R is to decrease tangential velocity.

Table 1 shows the effects of changing M^2, R and R_1 on the induced radial electric field (χ), the shear stress and torque at each disk ($g'(0)$ and $g'(1)$), and the lift force and edge pressure (A). Increasing M^2 increases χ, $g'(0)$, $g'(1)$ and A. Increasing the rotational Reynolds number (R_1) decreases the electric field, shear stress and torque at the lower disk, as well as decreasing the lift force and edge pressure; however, the shear stress and torque at the upper disk are increased. The effect of increasing the cross-flow Reynolds number R is, generally, the same as increasing R_1. However, the changes due to R are more dramatic for χ, $g'(0)$ and $g'(1)$ than the changes due to R_1. The reverse is true for A.

References

1. G. K. Batchelor, Note on a class of solutions of the Navier-Stokes equations representing steady rotationally symmetric flow, *Quart. J. Mech. Appl. Math.* **4**, 29 (1951).

2. K. Stewartson, On the flow between two rotating coaxial disks, *Proc. Camb. Phil. Soc.* **49**, 533 (1953).

3. G. N. Lance and M. H. Rogers, The axially symmetric flow of a viscous flow between two infinite rotating disks, *Proc. Roy. Soc. Lond.* **A266**, 109 (1962).

4. C. E. Pearson, Numerical solutions of the time dependent viscous flow between two rotating coaxial disks, *J. Fluid. Mech.* **21**, 623 (1965).

5. N. Rott and W. S. Lewellen, Flow between a rotating stationary disk, *Prog. Aero. Sci* **7**, 136 (1966).

6. G. L. Mekor, P. J. Chapple and V. K. Stokes, On the flow between a rotating and stationary disk, *J. Fluid Mech.* **31**, 95 (1968).

7. C. Y. Wang and L. T. Watson, Viscous flow between rotating discs with injection on the porous disc, *Z. Angew. Math. Phys.* **30**, 773 (1979).

8. A. C. Srivasthana and S. K. Sharma, The effect of a transverse magnetic field on the flow between two infinite disks, *Bull. Acad. Pol. Sci. (Ser. Sci. Tech.)* **9**, 639 (1961).

9. C. J. Stephenson, Magnetohydrodynamic flow between rotating coaxial disks, *J. Fluid Mech.* **38**, 335 (1969).

10. B. C. Chandrasekhara and N. Rudriah, Magnetohydrodynamic laminar flow between porous disks, *Appl. Sci. Res.* **23**, 42 (1970).

11. B. C. Chandrasekhara and N. Rudriah, Three dimensional MHD flow between two porous disks, *Appl. Sci. Res.* **25**, 179 (1971).

12. R. S. Agarwal and R. Bhargava, A numerical study of the flow between a rotating and a stationary porous coaxial disk, *Proc. Ind. Acad. Sci.* **88A**, 399 (1979).

13. M. W. Heruska, Micropolar flow past a porous stretching sheet, *M. S. Thesis*, Dept. of Computer Science, Virginia Polytechnic Institute and State University, Blacksburg, VA, Oct., (1984).

14. J. J. Moré, B. S. Garbow and K. E. Hillstrom, *User Guide for MINPACK-1*, ANL-80-74, Argonne National Laboratory, (1980).

15. L. F. Shampine and M. K. Gordon, *Computer Solution of Ordinary Differential Equations*, W. H. Freeman, San Francisco, (1975).

Figure Captions.

Figure 1. Effect of M^2 on flow field with $R = 2$, $R_1 = .447$ and $M^2 = 0, 16, 64, 256, 512$ (short dash, dotted, solid, long dash, dash dot). (a) Axial velocity $f(\varsigma)$. (b) Radial velocity $f'(\varsigma)$. (c) Tangential velocity $g(\varsigma)$.

Figure 2. Effect of R_1 on flow field with $M^2 = 16$, $R = 2$ and $R_1 = 2, 4, 10, 16$ (short dash, dotted, solid, long dash). (a) Axial velocity $f(\varsigma)$. (b) Radial velocity $f'(\varsigma)$. (c) Tangential velocity $g(\varsigma)$.

Figure 3. Effect of R on flow field with $M^2 = 16$, $R_1 = 2$ and $R = 2, 4, 10, 16$ (short dash, dotted, solid, long dash) (a) Axial velocity $f(\varsigma)$. (b) Radial velocity $f'(\varsigma)$. (c) Tangential velocity $g(\varsigma)$.

1a

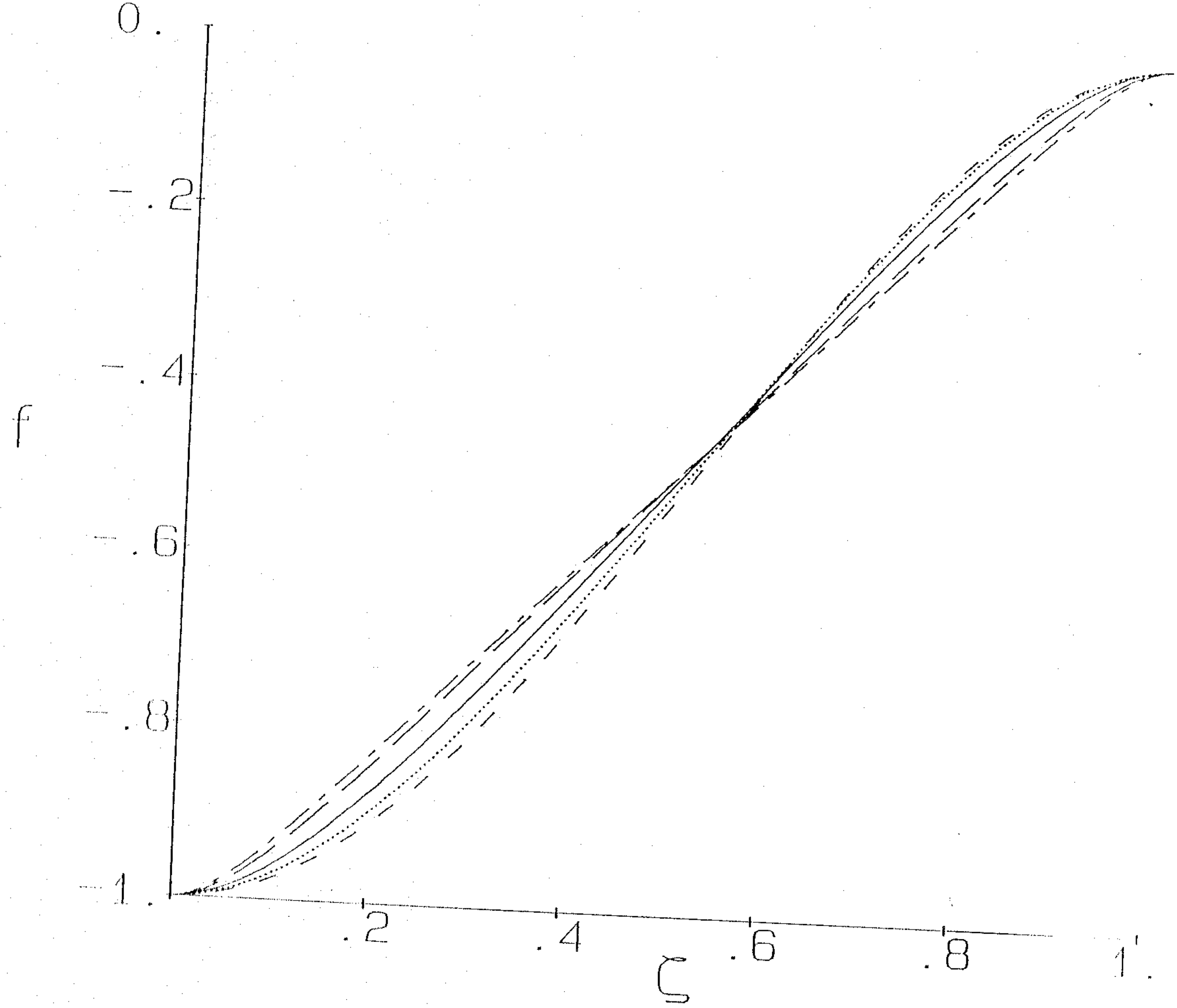

Figure 1a

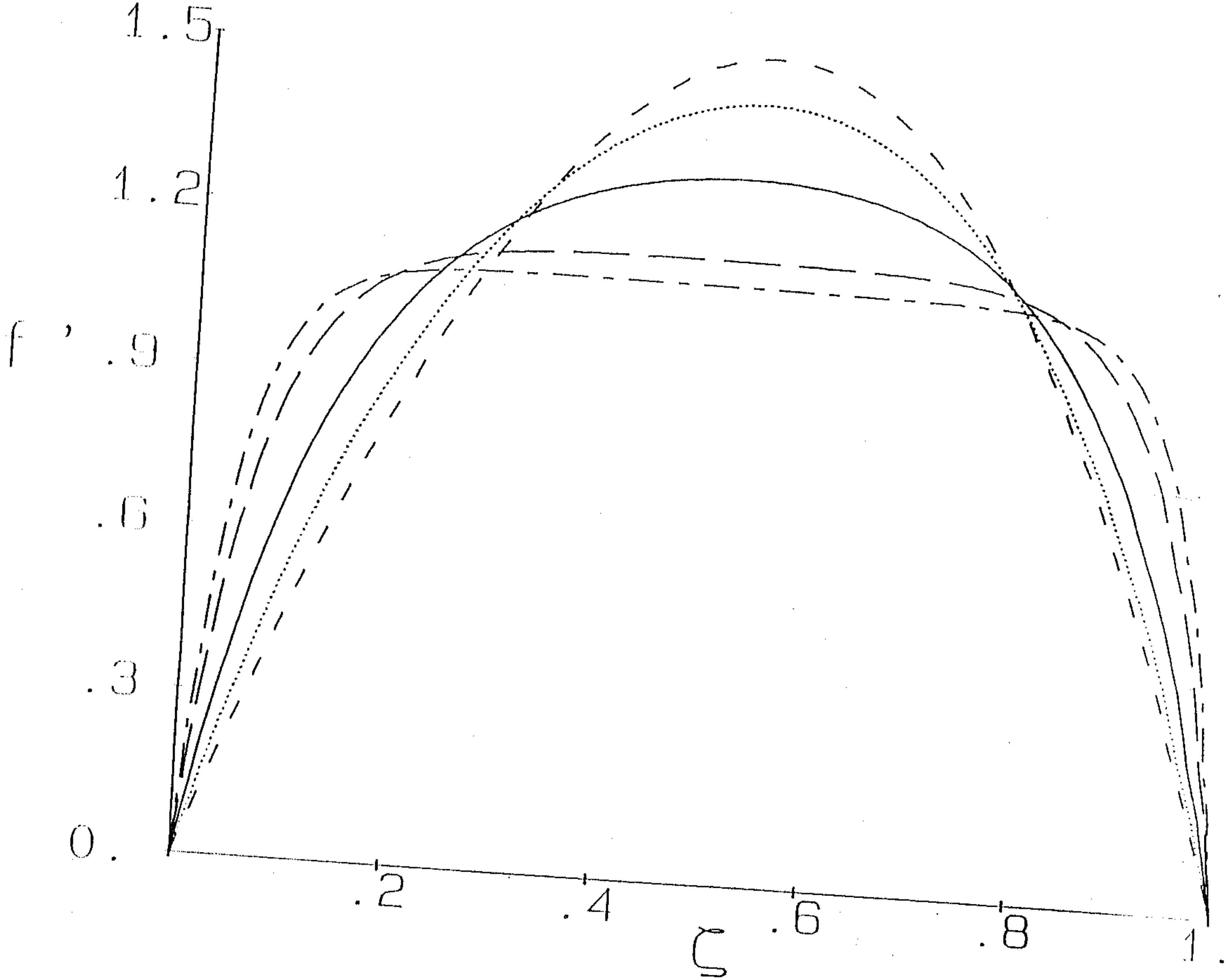

Figure 1b

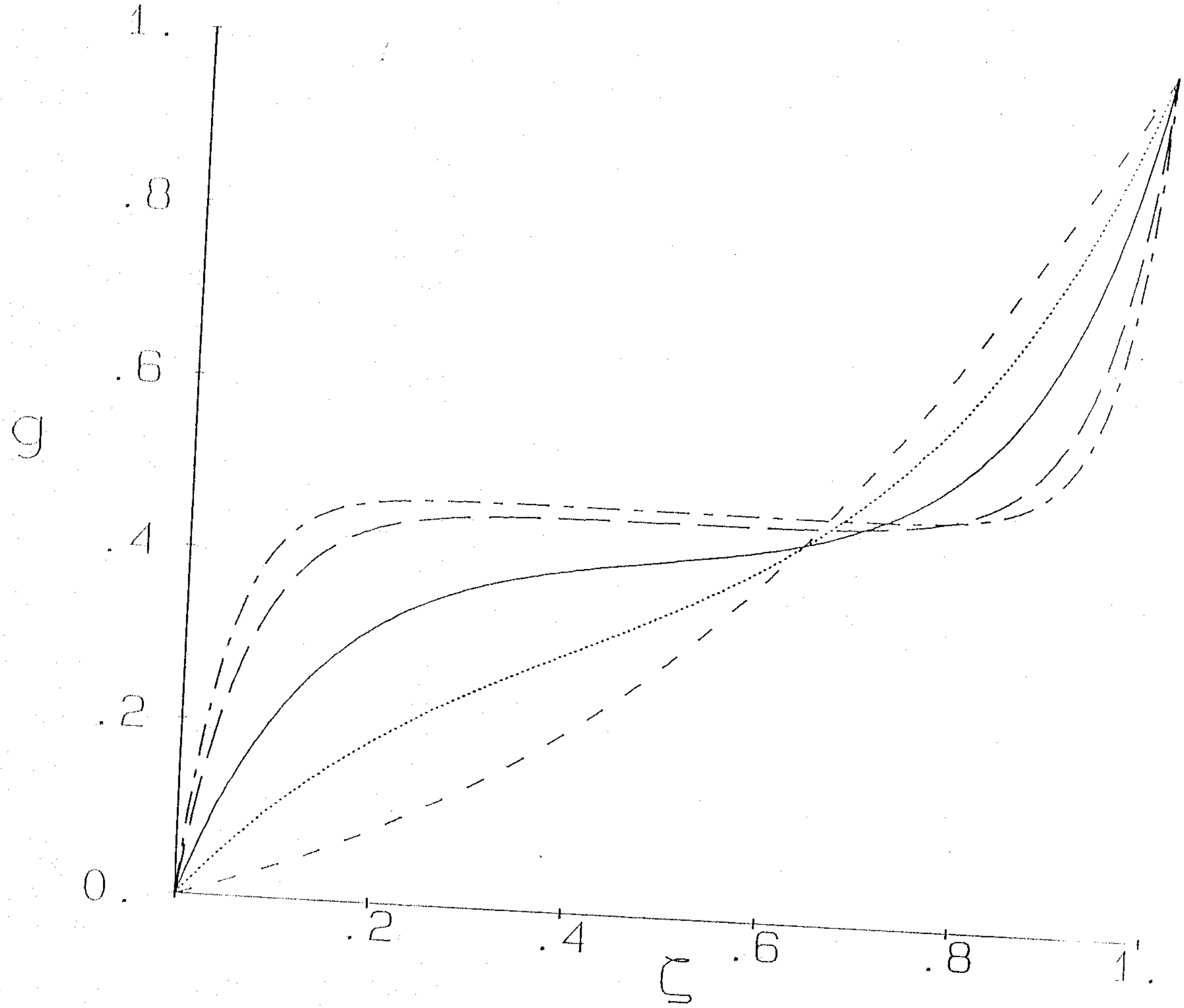

Figure 1c

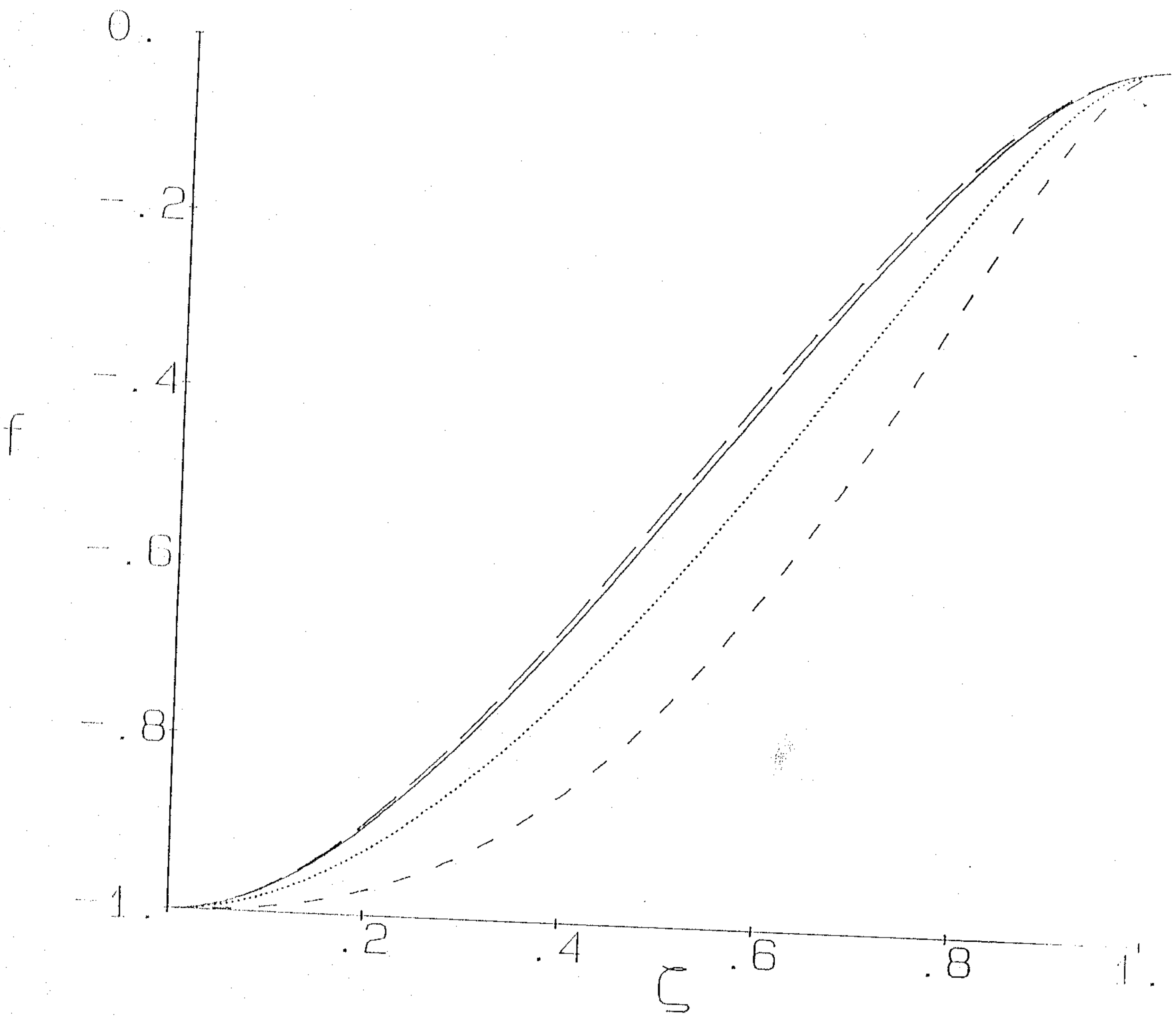

Figure 2a

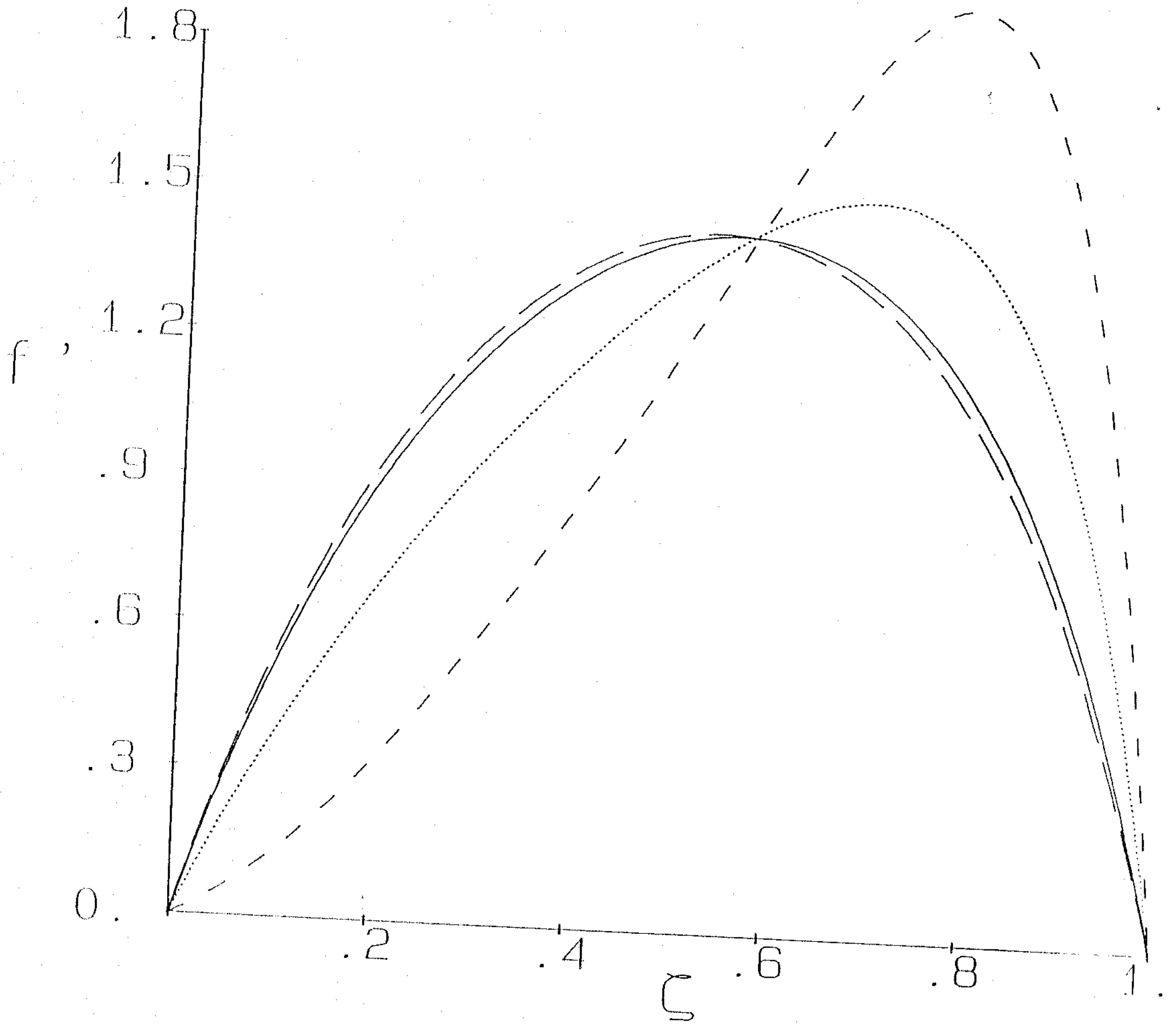

Figure 2b

2c

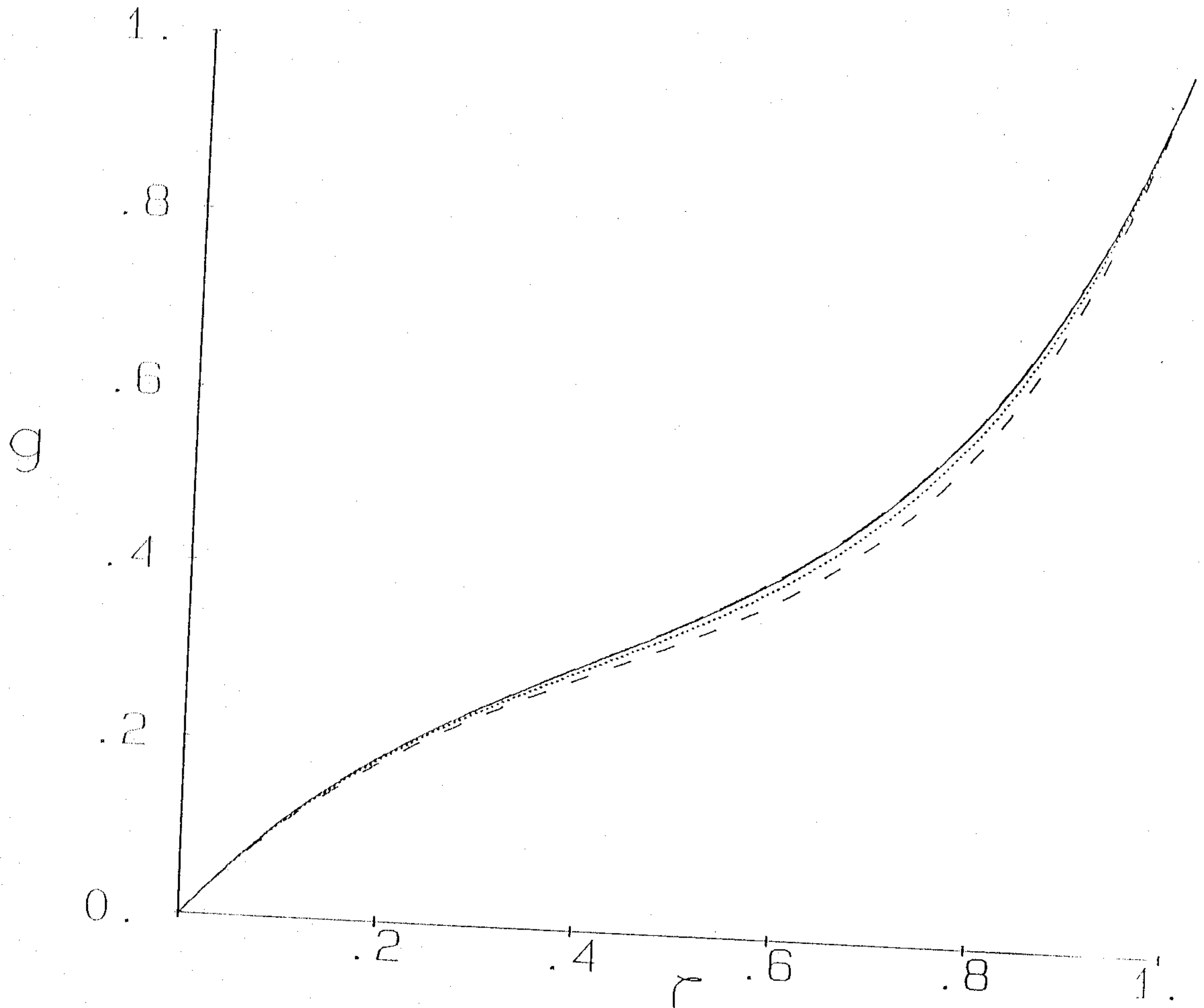

Figure 2c

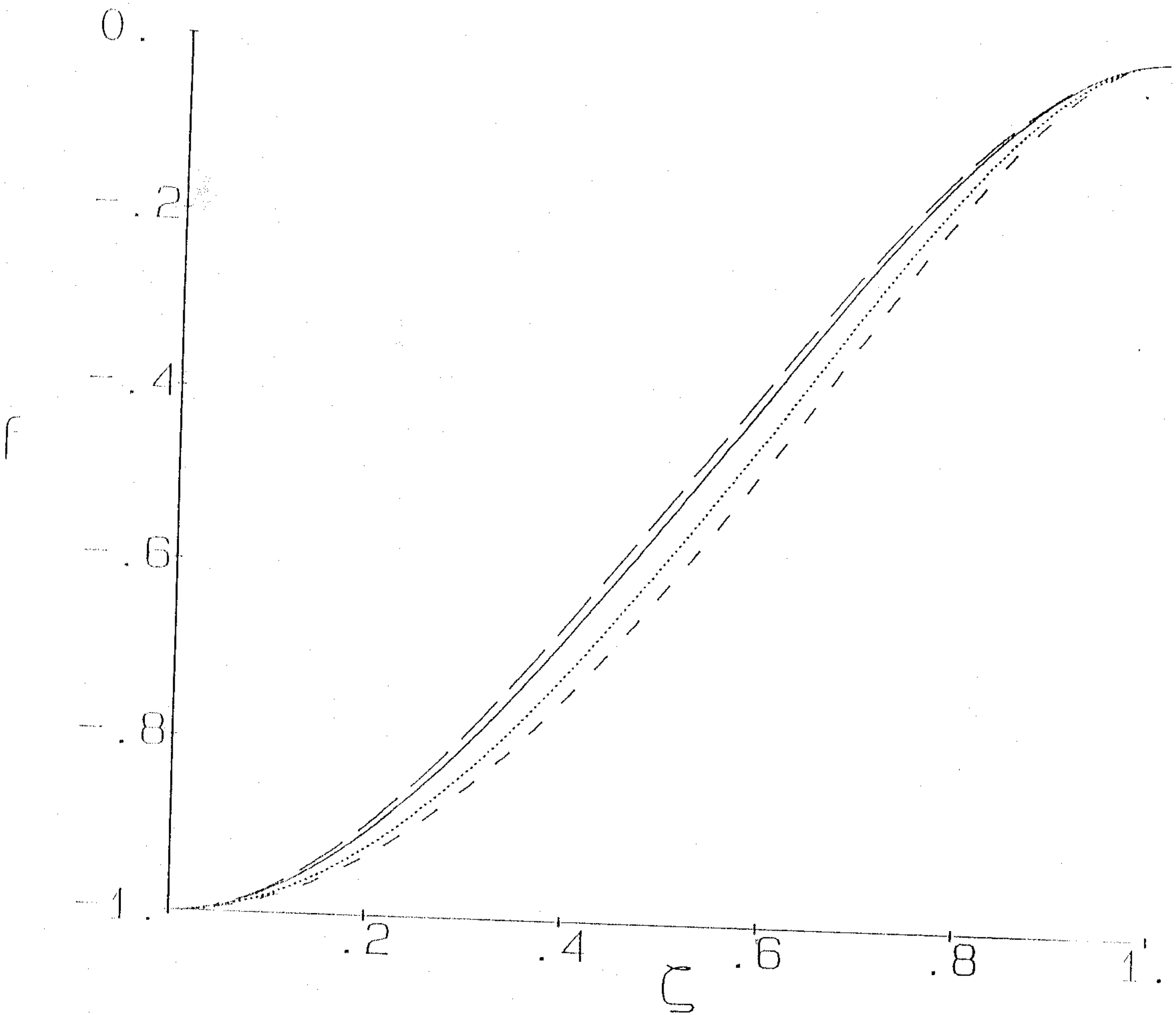

Figure 3a

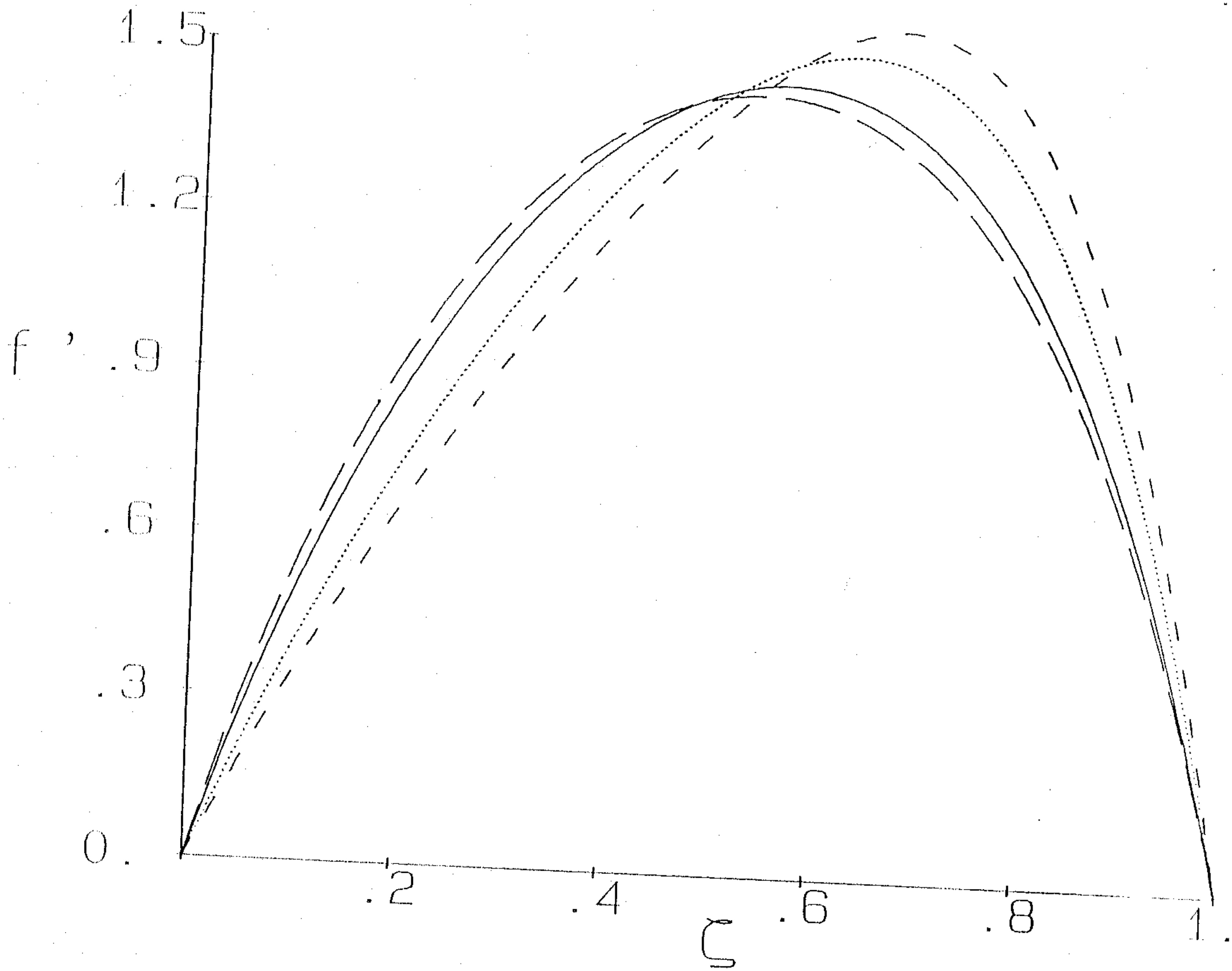

Figure 3b

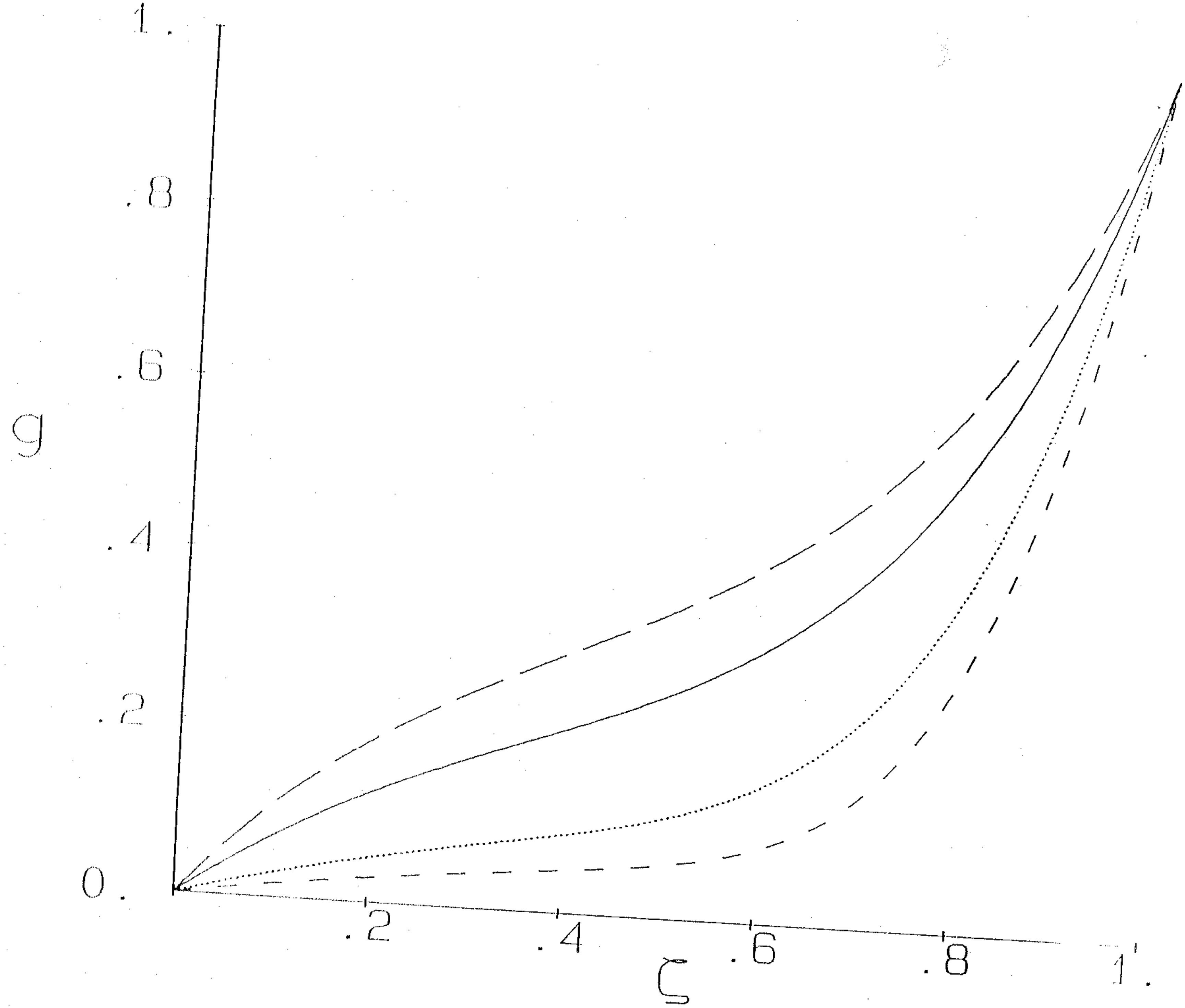

Figure 3c